Available online at www.sciencedirect.com

SCIENCE DIRECT®

Lithos 81 (2005) 235–254

LITHOS

www.elsevier.com/locate/lithos

Geochemistry of granitoids and their minerals from Rebordelo–Agrochão area, northern Portugal

M.E.P. Gomes[a,*], A.M.R. Neiva[b]

[a]Department of Geology, University of Trás-os-Montes and Alto Douro, 5000-911 Vila Real, Portugal
[b]Department of Earth Sciences, University of Coimbra, 3000-272 Coimbra, Portugal

Received 19 February 2004; accepted 15 November 2004
Available online 30 December 2004

Abstract

Deformed Hercynian peraluminous granitoids ranging from tonalite to granite crop out in the Rebordelo–Agrochão area, northern Portugal and some of them contain tonalitic and granodioritic enclaves. Variation diagrams of major and trace elements of the rocks, biotites and sphenes show fractionation trends. The most- and the least-deformed samples of granite and their biotites also define fractionation trends. There is decrease in all rare earth element (REE) contents and increase in the Eu anomaly in REE patterns from the most- to the least-deformed samples of granite. All the granitoids define a whole-rock Rb–Sr errorchron. A whole-rock Rb–Sr isochron for the least-deformed samples of granite yields an age of 357±9 Ma and an initial $^{87}Sr/^{86}Sr$ ratio of 0.7087±0.0007. Geochemical modelling suggests that the tonalitic magma evolved by AFC (fractional crystallization of magnesiohornblende, plagioclase, quartz, biotite and ilmenite, and assimilation of metasediments) to originate tonalitic and granodioritic enclaves, granodiorite and granite. $\delta^{18}O$ values support this mechanism. The tonalite is hybrid and derived by interaction of a mantle-derived magma and crustal materials.

Keywords: Granitoids; Microgranular enclaves; Deformation; Fractional crystallization; Assimilation

1. Introduction

At the Iberian massif, there is a well-exposed cross section of continental crust affected by the Variscan collision during the late Paleozoic that generated large volume of granites (Matte, 1986). Based on tectonics–magmatism relationships, Iberian Variscan granitoids have been classified in three major groups: pre-tectonic, syn- to late-tectonic and post-tectonic granites (Ferreira et al., 1987; Neiva and Gomes, 2001), using the last ductile deformation phase D3 criteria. Biotite-rich granitoids are syn- and late-D3 (Dias et al., 2002).

In northern and central Portugal, two-mica S-type granites predominate; biotite I-type granite is rare, but biotite and biotite–muscovite hybrid granites occur in

* Corresponding author. Fax: +351 259350480.
E-mail address: mgomes@utad.pt (M.E.P. Gomes).

0024-4937/$ - see front matter © 2004 Elsevier B.V. All rights reserved.
doi:10.1016/j.lithos.2004.11.001

several areas and generally contain microgranular enclaves (Neiva and Gomes, 2001). Some Portuguese hybrid granite compositions were modelled as derived from magma mixing of a mafic and a granite magma (Dias and Leterrier, 1994; Azevedo and Nolan, 1998; Silva et al., 2000), from fractional crystallization of a granite magma and assimilation of country pelitic sediments (Silva and Neiva, 2000), and also of marbles (Neiva, 1981).

This paper presents the geology, petrography, mineralogy, geochemistry and isotopic data of hybrid Hercynian granitoids from Rebordelo–Agrochão area, northern Portugal to study their petrogenesis. Data were used to test specific involved magmatic processes.

2. Geological setting

The Rebordelo–Agrochão area (Fig. 1a) is located in the Galiza and Trás-os-Montes Zone of the Iberian Terrane (Ribeiro et al., 1990), which belongs to the lower Silurian of the parautochthonous domain, the so-called Peritransmountain subdomain (Ribeiro, 1974).

The granitoids from Rebordelo–Agrochão area intruded concordantly Silurian metasediments that consist essentially of quartzites, phyllites and graphite schists, and were deformed by three Hercynian deformation phases: D1, D2 and D3. The regional metamorphism reached maximum conditions of 450 °C and 6–7 kb (Lécolle et al., 1981). The studied granitoids are: fine-grained slightly porphyritic biotite–hornblende tonalite B1, fine- to medium-grained porphyritic biotite granodiorite B2, and medium- to coarse-grained porphyritic biotite–muscovite granite B3 (Fig. 1b), which are deformed by D3.

The tonalite B1 crops out as a small-elongated NW–SE body, and is surrounded by the biotite–muscovite granite B3. The biotite granodiorite B2 occurs as four small bodies inside the granite B3, which is the most abundant. The contacts between granodiorite and granite are lobate.

Field evidence, such as magmatic structures given by foliation and lineation, which are recognized macroscopically, preferred orientations of K-feldspar phenocrysts and biotite; submagmatic microstrutures shown by intracrystalline fractures filled with other minerals; and solid state deformation presented by S–C structures, suggest that the emplacement of the granitoid magmas may have taken place before the Variscan deformation phase D3. The granite shows heterogenous deformation with magmatic flow foliation defined by planar orientation of generally visible

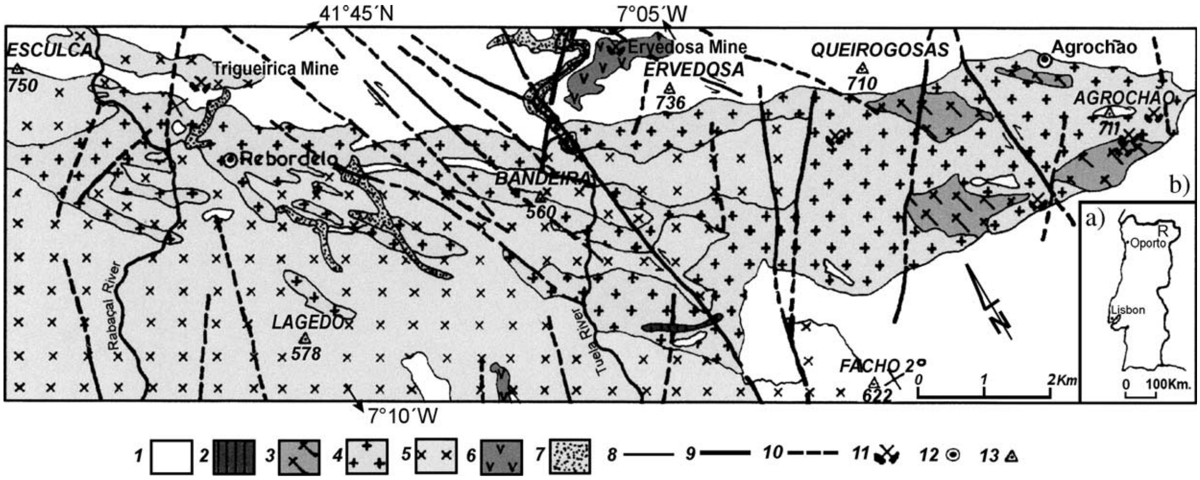

Fig. 1. (a) Location of the Rebordelo–Agrochão area (R), northern Portugal. (b) Geological map of this area. 1—Silurian schists, 2—fine-grained slightly porphyritic biotite–hornblende tonalite B1, 3—fine- to medium-grained porphyritic biotite granodiorite B2, 4—medium- to coarse-grained porphyritic biotite–muscovite granite B3, 5—medium-grained muscovite–biotite granite, 6—fine- to medium-grained muscovite granite, 7—alluvium, 8—geologic contact, 9—fault, 10—probable fault, 11—Sn, W abandoned mines, 12—village, 13—geodesic point.

K-feldspar phenocrysts within sheared bands, which have well-developed subparallel S–C type structures to the Laza–Rebordelo dextral shear zone in the central and NW part of the massif.

The granodiorite and granite have microgranular enclaves of biotite tonalite and granodiorite compositions, and rare xenoliths of country rocks, which are commonly observed close to the contacts with the NW border of the massif. The microgranular enclaves are fine-grained, and darker in colour than host granitoids. Fine- to medium-grained biotite tonalite E1 and medium- to fine-grained biotite granodiorite E2 enclaves were distinguished. They are rounded or ovoid, but they became irregular, fusiform and elongated in the shear bands. In general, they are 20–30 cm in diameter, but can range from 5 cm to 1 m.

The granitoids produced contact metamorphism consisting of an outer zone, 1 to 2 km wide, of biotite schist, and an inner zone, 0.2 to 0.5 km wide, of hornblende hornfels containing sillimanite, andalusite and rare cordierite. The granitoids were intruded by 328–315 Ma muscovite–biotite granites or muscovite granite and the contacts are sharp. Some aplite, pegmatite and aplite–pegmatite veins cut mainly the granite and occur dominantly close to the contact with metasedimentary rocks. N–S and NNE–SSW faults, younger than D3, were penetrated by quartz veins, and cut granites and surrounding country rocks. Some of them have tin and tungsten minerals and sulphides. Cassiterite and stannite were exploited at the Ervedosa mine and cassiterite, wolframite and scheelite were exploited at the Trigueiriça and Agrochão mines.

3. Petrography

All granitoids contain quartz, microperthitic K-feldspar, plagioclase, biotite, chlorite (after biotite), sphene, apatite, ilmenite, zircon and rutile. They have tourmaline and monazite, except the biotite–hornblende tonalite, which is the only one containing amphibole, allanite and magnetite. Some samples of granodiorite and granite have primary muscovite. Granite also contains sillimanite. The modal compositions are given in Table 1. Following the classification of Le Bas and Streckeisen (1991), there are biotite–hornblende tonalite (B1), biotite tonalite enclave (E1), biotite granodiorite enclave (E2), biotite granodiorite (B2) and biotite–muscovite granite (B3) as shown in Fig. 2 and Table 1.

The tonalite has a subhedral granular texture and contains rare small 30×12 mm K-feldspar phenocrysts and oligoclase–labradorite (An_{28}–An_{60}) phenocrysts up to 12×8 mm. The microgranular enclaves and granodiorite show a porphyritic seriate texture, contain oligoclase–labradorite (An_{26}–An_{54}) phenocrysts; granodiorite also has K-feldspar phenocrysts up to 100×60 mm. The granite has a porphyritic subhedral granular texture with phenocrysts of K-feldspar and rare of albite–andesine (An_5–An_{32}) ranging from 30×15 to 150×60 mm.

Quartz crystals are xenomorphic with strong undulatory extinction and progressive granulation to the borders; locally, there are recrystallized granular aggregates with lenticular ribbons. Quartz presents several generations and contains inclusions of all minerals, particularly biotite, sillimanite, apatite and ore minerals.

Microperthitic orthoclase and microcline phenocrysts are hypidiomorphic to xenomorphic with rounded and smooth margins in the most-deformed granitoids. In general, there are micas and small later plagioclase crystals at the borders of K-feldspar cystals. Some of the large K-feldspar crystals are broken and the fractures are filled with quartz, plagioclase, chlorite, epidote and calcite. Orthoclase crystals are twinned according to the Carlsbad law and microcline crystals are often cross-hatch twinned. The matrix K-feldspar is microperthitic and intersticial, showing better defined crosshatched twinning than that in the phenocrysts. K-feldspar contains inclusions of biotite, muscovite, apatite and opaque minerals.

Plagioclase phenocrysts are hypidiomorphic, but locally are xenomorphic, polysynthetically twinned, with borders surrounded by other minerals. The twin planes of plagioclase are curved and the crystals have undulatory extinction and transversal microfractures in the most-deformed granitoids. In general, plagioclase is strongly zoned. The phenocryst compositions were already given. The matrix plagioclase is oligoclase–labradorite in tonalites, albite–andesine in granodioritic rocks and albite-oligoclase in granite. Plagioclase has inclusions of biotite, muscovite, chlorite, quartz and apatite. Quartz-albite band and myrmekite intergrowths are often found at the K-

Table 1
Modal compositions and average chemical analyses (oxides in wt.%, trace and rare earth elements in ppm) of granitoids from Rebordelo–Agrochão, northern Portugal

	B1	E1	E2	B2		B3		(a)	(b)
Samples	*n*=3	*n*=2	*n*=2	*n*=7	σ	*n*=18	σ	*n*=2	*n*=3
Quartz	25.8	32.6	31.7	30.7	2.4	28.1	6.5	22.2	29.5
Plagioclase	43.9	39.6	39.1	41.5	3.9	30.7	3.5	31.9	36.4
K-feldspar	5.3	0.5	9.0	10.1	4.2	26.8	9.5	28.1	20.2
Amphibole	1.1	–	–	–	–	–	–	–	–
Biotite	22.3	26.7	19.9	16.4	1.7	10.8	3.6	14.4	9.6
Muscovite	–	0.4	0.3	0.7	1.0	2.8	1.6	1.9	3.7
Other minerals	1.6	0.2	–	0.6	0.3	0.8	0.5	1.5	0.6
SiO_2	61.88	65.54	65.78	66.56	1.47	69.18	1.18	67.83	70.88
TiO_2	0.81	0.78	0.69	0.72	0.07	0.51	0.07	0.60	0.40
Al_2O3	16.57	15.84	16.22	15.59	0.44	15.44	0.44	15.80	15.08
Fe_2O_3	0.93	0.25	0.89	0.39	0.18	0.32	0.28	0.44	0.09
FeO	4.28	4.25	3.12	3.60	0.32	2.45	0.45	2.98	2.01
MnO	0.22	0.19	0.18	0.20	0.02	0.11	0.01	0.11	0.11
MgO	3.12	2.13	1.92	1.67	0.43	1.04	0.16	1.27	0.81
CaO	3.94	3.06	2.56	2.63	0.48	1.72	0.28	2.10	1.36
Na_2O	2.96	3.94	2.69	3.10	0.28	3.41	0.24	3.32	3.29
K_2O	3.81	2.78	4.21	4.37	0.54	4.75	0.54	4.52	5.05
P_2O_5	0.37	0.28	0.27	0.29	0.05	0.28	0.04	0.29	0.23
H_2O+	0.68	0.59	1.02	0.50	0.10	0.55	0.16	0.48	0.48
H_2O-	0.11	0.09	0.26	0.13	0.07	0.14	0.06	0.13	0.13
Total	99.68	99.72	99.81	99.75		99.90		99.87	99.92
Cl	365	339	416	295	59	309	69	356	296
F	1219	2109	985	1257	100	1279	195	1548	1420
Cr	71	75	63	46	18	35	9	42	28
V	99	79	64	74	11	44	9	58	30
Nb	18	15	19	19	2	18	2	16	19
Sn	42	52	62	47	29	56	12	54	57
Zn	83	84	73	69	5	61	9	71	52
Li	156	165	162	148	25	143	32	187	156
Ni	27	34	18	12	6	7	3	8	3
Zr	335	317	291	285	13	217	31	257	166
Cu	22	19	22	13	6	9	9	8	10
Sc	16	7	11	9	3	6	3	8	5
Y	59	53	55	58	3	54	3	55	50
Sr	278	189	225	208	25	150	20	165	129
Pb	22	4	20	17	7	25	5	24	28
Ba	642	329	685	659	55	465	106	483	431
Rb	207	256	244	251	27	282	19	293	295
Cs	16	8	9	8	5	24	10	23	16
W	11	6	7	*	*	*	*	–	*
U	*	4	*	8	*	11	7	12	12
Th	20	24	21	16	7	16	6	25	12
Hf	8	8	7	7	*	6	1	7	5
La	95.90	69.40	69.20	75.90		45.50	8.14	52.70	32.30
Ce	156.80	133.10	124.50	122.50		100.36	20.65	120.70	68.70
Nd	75.20	61.20	56.00	58.20		48.22	8.73	58.10	35.40
Sm	7.49	6.17	6.46	7.53		9.00	1.70	10.50	6.28
Eu	1.46	1.14	1.28	1.11		0.86	0.09	0.98	0.73
Gd	11.04	11.38	11.52	10.60		6.76	1.55	8.20	4.50
Tb	0.99	0.82	0.96	1.03		0.90	0.15	1.09	0.72
Yb	2.50	1.50	1.30	1.20		2.28	0.37	2.72	1.84
Lu	0.41	0.23	0.34	0.43		0.27	0.05	0.35	0.22

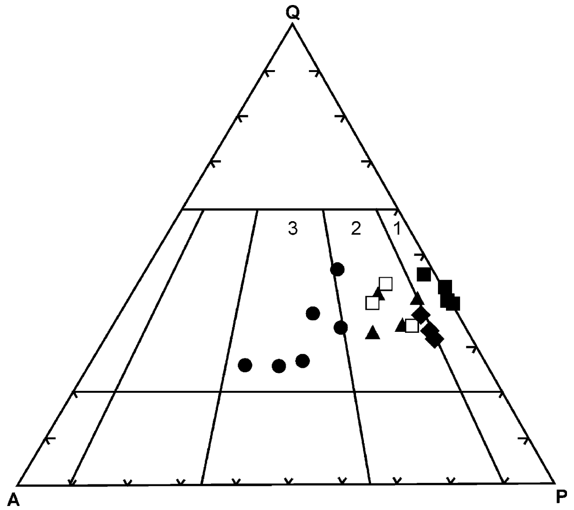

Fig. 2. Q–A–P diagram of Le Bas and Streckeisen (1991) with granitoid rocks from Rebordelo–Agrochão area. Symbols: ◆—tonalite B1, ■—tonalitic enclave E1, □—granodioritic enclave E2, ▲—granodiorite B2, ●—granite B3. Fields: 1—tonalite, 2—granodiorite, 3—monzogranite.

feldspar–plagioclase contacts. Later oligoclase (An_{13}) was found in microshear bands in the most-deformed granite samples.

Amphibole was only found in tonalite. It is xenomorphic and pleochroic from brownish green (α), green (β) to light green (γ). Some crystals are slightly zoned with the core darker than the rim; $2V_x=78\pm2°$. In general, it occurs in elongated amphibole-rich polycrystalline aggregates, such as clots, with minor amounts of biotite, ilmenite, plagioclase and sphene. The biotite is hypidiomorphic and pleochroic from γ, β=dark reddish brown to α=pale yellow. In the deformed granite, the biotite is weakly to intensively bent, fragmented with undulatory extinction or there is another generation of later biotite associated with quartz and feldspars in the shear bands. Biotite contains inclusions of zircon, sphene, apatite, ilmenite and rutile. The chlorite is after biotite and scarce in enclaves and granodiorite. It is pleochroic from γ, β=dark green to α=light green. Muscovite is also subhedral and is rare in the enclaves and granodiorite. Primary muscovite only occurs in granodiorite and granite, but is always less abundant than biotite. In the deformed granite samples, muscovite has similar optical characteristics to those of biotite.

Sillimanite was only identified in some samples of granites, close to the contact with country rock. Apatite is the most abundant accessory mineral, occurring as large crystals in granite and as small prismatic and acicular crystals in enclaves. Zircon and sphene occur in all granitoids. Monazite, tourmaline and fluorite are common in the granite, while allanite and magnetite only occur in the tonalite.

4. Analytical methods

The major elements of minerals were determined using a Modified Cambridge Geoscan electron microprobe with Link Systems energy-dispersive system at Manchester University, U.K., and a Cameca Camebáx at Portuguese Laboratories of IGM, Oporto. The micas were separated with a magnetic separator and heavy liquids in order to be analysed for their trace elements. The purity estimated by petrographic examination of the mineral separates is ~99.8%. The main contaminants are zircon, sphene and apatite.

The major and trace elements of granites and trace elements of micas were determined by X-ray fluorescence (XRF) at Manchester University, using the method of Brown et al. (1973), with precisions better than ±1% for the major elements and Rb and of ±4% for the other trace elements. Rare earth elements (REE), U, Th, Ta and Hf of granitoids were determined by neutron activation at the Imperial College Reactor Center, Ascot, U.K., with a precision of about ±5%.

Total Fe_2O_3 of biotites, and Li of rocks and micas were determined by atomic absorption with a precision of about ±2%. FeO of granites was determined by titration with a standardized potassium permanganate solution, while H_2O+ was determined using a Penfield tube; the precision was about ±1%. F was determined by selective ion electron analysis with a precision of about ±2%. These determinations were carried out at

Note to Table 1:
B1—tonalite, E1—tonalitic enclave, E2—granodioritic enclave, B2—granodiorite, B3—granite, (a) the most-deformed granite B3, (b) the least-deformed granite B3, *n*—number of analysed samples, σ—standard deviation, – not detected, *below the limit of sensitivity. Analyst: M.E.P. Gomes.

the Department of Chemistry, University of Trás-os-Montes and Alto Douro, Vila Real, Portugal.

The radiometric determinations were carried out at the Department of Earth Sciences, University of Oxford, U.K. Sr was separated by a conventional ion exchange technique (Pankhurst and O'Nions, 1973) and isotopically analysed on single Ta filaments on a VG-Micromass 54E spectrometer. The $^{87}Sr/^{86}Sr$ ratios have been corrected for mass fractionation by normalizing to $^{87}Sr/^{86}Sr$=0.837521. The standard used was the NBS987 and gave a repeated value of $^{87}Sr/^{86}Sr$=0.710260±0.000025. This is within error and no correction is necessary to the sample results. 2σ error on $^{87}Sr/^{86}Sr$ ratios is about 0.005%. Rb and

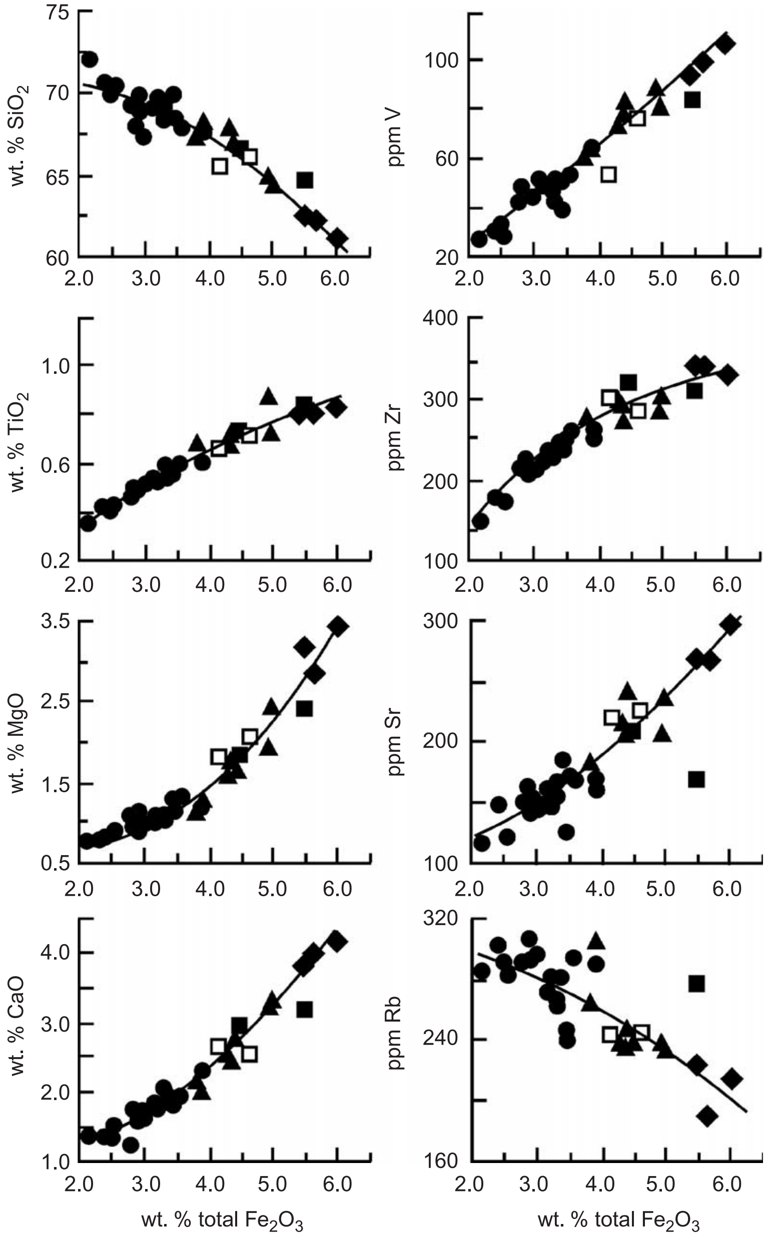

Fig. 3. Variation diagrams for selected major and trace elements of granitoids from Rebordelo–Agrochão area. Symbols as in Fig. 2.

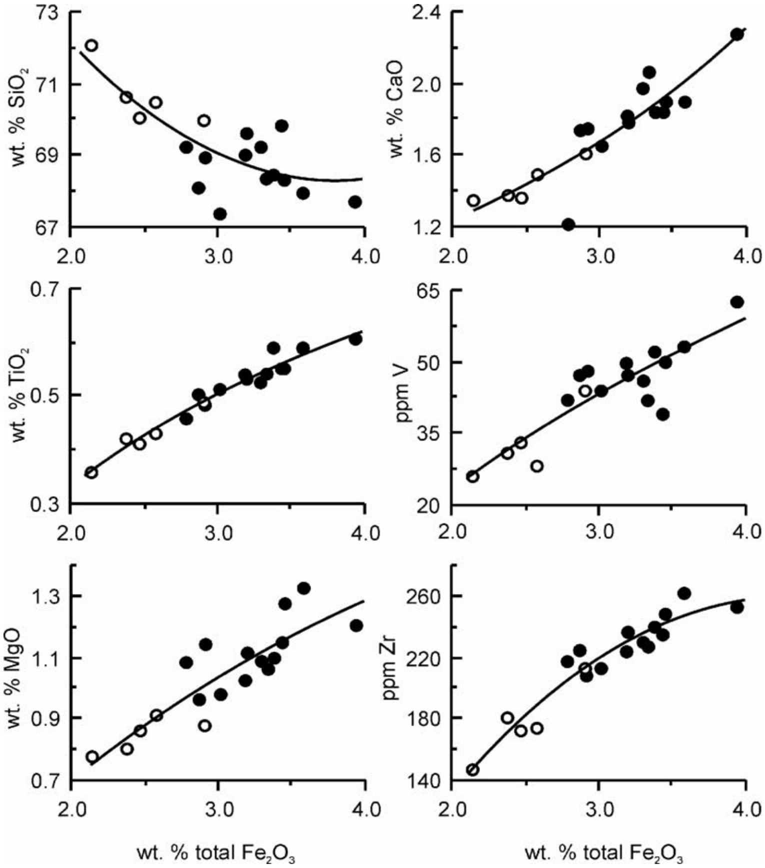

Fig. 4. Variation diagrams for selected major and trace elements of the most-deformed and the least-deformed samples of the granite B3 from Rebordelo–Agrochão area. Symbols: ●—the most-deformed samples, and ○—the least-deformed samples.

Sr have been determined on pressed powder pellets by XRF with precision about ±1%. Rb and Sr contents, computed with absorption coefficients obtained from Compton scatter peak intensities, are precise to better than ±5%. Regression lines have been calculated using the least-squares method as implemented in the Isoplot program (Ludwig, 1990). Sm and Nd ppm have been determined by isotope dilution and the

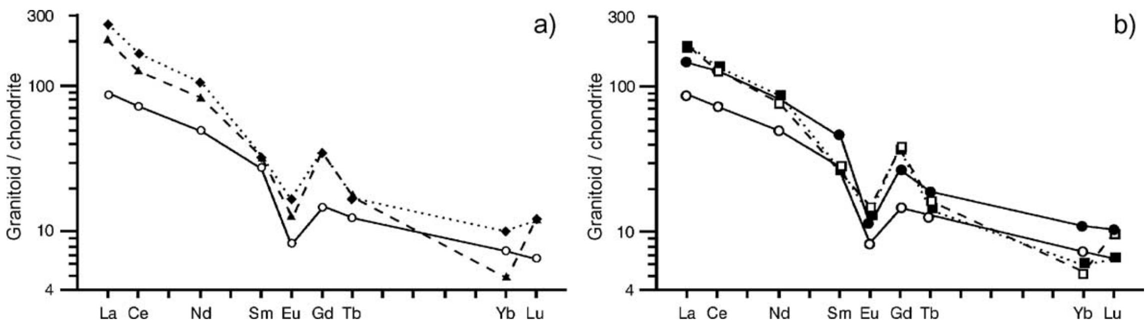

Fig. 5. Chondrite-normalized REE abundances of the biotite granitoids from Rebordelo–Agrochão area: (a) average of tonalite and granodiorite and the least-deformed sample of granite; (b) enclaves and the least-deformed and the most-deformed samples of the host granite. Symbols as in Figs. 2 and 4. Furthermore, in (a) ..... B1, - - - B2, —B3,(b) ..... E1, - - - E2 and —B3. Chondrite abundances from Haskin et al. (1968).

Table 2
Rb–Sr isotopic analyses of granitoids from Rebordelo–Agrochão, northern Portugal

	Rb (ppm)	Sr (ppm)	Rb/Sr	$^{87}Rb/^{86}Sr$	$^{87}Sr/^{86}Sr$	±error	$(^{87}Sr/^{86}Sr)_{357Ma}$
Tonalite B1							
156	212.2	298.4	0.704	2.0389	0.71740	0.00003	0.7070
155	222.0	268.0	0.822	2.3798	0.71950	0.00003	0.7074
Tonalitic enclave E1							
5D	235.7	208.7	1.125	3.2598	0.72510	0.00003	0.7085
Granodioritic enclave E2							
2D	243.6	221.0	1.096	3.1756	0.72430	0.00003	0.7082
Granodiorite B2							
132	232.0	235.3	0.979	2.8373	0.72150	0.00003	0.7071
18A	234.5	205.6	1.136	3.2924	0.72528	0.00003	0.7085
80	244.8	241.4	1.007	2.9158	0.72130	0.00004	0.7065
108	264.5	182.8	1.444	4.1868	0.72921	0.00003	0.7079
18	236.0	213.9	1.098	3.1817	0.72392	0.00003	0.7077
16	306.1	172.9	1.768	5.1268	0.73280	0.00003	0.7067
Granite B3							
1	297.2	144.5	2.064	5.9912	0.73920	0.00003	0.7088
13	281.1	184.1	1.503	4.4162	0.73121	0.00007	0.7088
3	280.7	147.6	1.902	5.5128	0.73673	0.00003	0.7087
126	307.9	153.7	2.006	5.8219	0.73820	0.00004	0.7086
17	292.0	120.9	2.439	7.0827	0.74456	0.00004	0.7086
17E	284.2	119.5	2.402	6.9729	0.74442	0.00003	0.7090

Analyst: M.E.P. Gomes.

error on $^{147}Nd/^{144}Nd$ ratio was ±0.1%. The $^{143}Nd/^{144}Nd$ ratios were determined on a VG 54E mass spectrometer and corrected for within-run mass fractionation by normalization to a $^{146}Nd/^{144}Nd$=0.7219. The replicate analyses of La Jolla standard yielded $^{143}Nd/^{144}Nd$=0.511858±0.000029 (0.0056% 2σ). The model age T_{DM} (depleted mantle) have been calculated using the $^{143}Nd/^{144}Nd$=0.513114 and $^{147}Sm/^{144}Nd$=0.222 from Michard et al. (1985).

Oxygen isotope analyses of whole-rock samples were carried out at the Department of Earth Sciences, the University of Western Ontario, Canada, using conventional extraction line and employing chlorine trifluoride as the reagent.

5. Whole-rock geochemistry

Representative analyses of major and trace elements and rare earth element contents of granitoids are given in Table 1. All granitoids are peraluminous with the molecular ratio $Al_2O_3/(CaO+Na_2O+K_2O)$ of 1.00–1.22. Normative corundum ranges from 1.00 to 3.46. They display an alumino-cafemic evolutive trend from biotite–hornblende tonalite to biotite–muscovite granite, which may indicate an infra-crustal contribution on the origin of magma (Debon and Le Fort, 1983).

According to a geochemical classification proposed by Frost et al. (2001), these granitoids are magnesian

Table 3
Sm–Nd isotopic analyses of tonalite, tonalitic enclave and granite from Rebordelo–Agrochão, northern Portugal

	Sm (ppm)	Nd (ppm)	$^{147}Sm/^{144}Nd$	$^{143}Nd/^{144}Nd$	% Error	$(^{143}Nd/^{144}Nd)_{357Ma}$	εNd_{357Ma}	$T_{DM357Ma}$
Tonalite B1	9.081	53.645	0.1023	0.512198	0.0018	0.51194	−4.3	1.16
Tonalitic Enclave E1	9.667	60.820	0.0961	0.512169	0.0019	0.51194	−4.6	1.14
Granite B3	7.761	41.487	0.1131	0.512155	0.0018	0.51189	−5.6	1.34

T_{DM} age was calculated based on values of De Paolo (1981a). Analyst: M.E.P. Gomes.

Table 4
$\delta^{18}O$ values in ‰ and SiO_2 and total Fe_2O_3 in wt.% of selected samples of granitoids from Rebordelo–Agrochão, northern Portugal

	$\delta^{18}O$	SiO_2	Total Fe_2O_3
Tonalite B1			
156	8.60	61.05	5.97
155	9.08	62.39	5.49
Tonalitic enclave E1	9.91	66.47	4.47
Granodioritic enclave E2	9.81	66.12	4.61
Granodiorite B2			
132	9.30	64.31	4.97
16	9.69	67.98	3.92
Granite B3			
15	9.34	67.69	3.93
49	10.10	68.95	2.90
17A	9.74	72.04	2.15

Analyst: M.E.P. Gomes.

and dominantly alkalic–calcic. The biotite–hornblende tonalite is the richest in TiO_2, total Fe_2O_3, MgO, CaO, P_2O_5, V, Zr, Sr, La, Ce and Nd and the poorest in SiO_2, Sn and Rb (Table 1 and Fig. 3). The variation diagrams for selected major and trace elements of granitoids versus total Fe_2O_3 show curvilinear variation trends (Fig. 3) that indicate it is not restite unmixing and suggest a fractional crystallization model and may be interpreted in terms of sequential changes from biotite–hornblende tonalite to biotite–muscovite granite. The total Fe_2O_3 has been chosen as a differentiation index because it shows a better discrimination between these granitoid rocks than does SiO_2. In general, tonalitic and granodioritic enclaves plot close to these trends and have intermediate compositions between those of tonalite and host granite. Consequently, there is decrease in TiO_2, total Fe_2O_3, MgO, CaO, Cr, V, Zr and Sr and increase in SiO_2 and Rb from enclaves to the host granite, which is consistent with the fractional crystallization process.

The heterogeneous deformation of granite B3 identified by the geological and petrographical studies is expressed in the geochemical data (Table 1), which indicate that the most-evolved samples of granite are the least-deformed samples and are richer in SiO_2, K_2O and poorer in TiO_2, total Fe_2O_3, MgO, CaO, Cr, V, Zn, Li, Zr, Sr, Ba and all rare earth elements than the most deformed samples of granite (Table 1, Figs. 4 and 5b) due to fractional crystallization.

The chondrite-normalized REE patterns of tonalite, granodiorite and granite are generally subparallel (Fig. 5a). $\sum$REE (352–151) and LREE (La_N/Sm_N=7.34–2.95) decrease, while the negative Eu anomaly (Eu/Eu*=0.44–0.40) increases from tonalite to granite (Fig. 5a). The rare earth element patterns for the most-deformed sample and the least-deformed sample of granite are subparallel and there is a decrease in all rare earth elements and increase in the negative Eu anomaly from the former to the latter (Fig. 5b).

6. Isotopic data

Isotopic analytical data are presented in Tables 2–4. Two samples of tonalite B1, three samples of granodiorite B2 and six samples of granite B3 define a whole-rock Rb–Sr isochron, which yields an age of 386±9 Ma and an initial $^{87}Sr/^{86}Sr$ ratio of 0.7063±0.0005 (Fig. 6a). These samples and the tonalitic and granodioritic enclaves E1 and E2 fit a

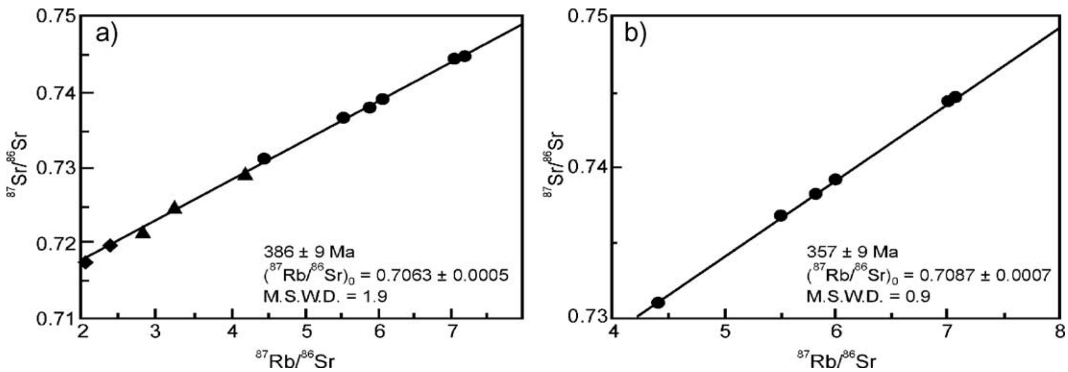

Fig. 6. Whole-rock Rb–Sr isochron of granitoids from Rebordelo–Agrochão area: (a) B1, B2 and B3; (b) B3 host granite. Symbols as in Fig. 2.

Table 5
Compositions of feldspars of granitoids from Rebordelo–Agrochão, northern Portugal

Rock type	B1	E1	E2	B2	B3	(a)	(b)
Plagioclase (An content)							
Phenocrysts	60–28	54–26	–	54–27	32–5	32–17	19–5
Matrix	53–27	43–26	40–20	34–1	27–3	25–3	18–1
K-feldspar (Or content)							
Phenocrysts	–	–	88	89–91	82–90	85–88	88–90
Matrix	91–94	94	87–89	91–96	89–96	92–96	94–95
K-feldspar (wt.% BaO)							
Phenocrysts	–	–	0.33	0.26	0.38	0.38	n.a.
Matrix	1.19	n.a.	0.12	0.21	0.22	0.22	n.a.

B1—tonalite, E1—tonalitic enclave, E2—granodioritic enclave, B2—granodiorite, B3—granite, (a) the most-deformed granite B3, (b) the least-deformed granite B3, n.a.—not analysed, Analyst: M.E.P. Gomes.

whole-rock Rb–Sr errorchron, which yields similar values of 386±9 Ma, initial $^{87}Sr/^{86}Sr$ ratio of 0.7067±0.0006, but with an M.S.W.D. of 2.9. Furthermore, three samples of granodiorite do not fit the whole-rock Rb–Sr isochron probably due to their high degree of deformation. The least-deformed samples of granite B3 fit a whole-rock Rb–Sr isochron, which yields a minimum emplacement age of 357±9 Ma and initial $(^{87}Sr/^{86}Sr)$= 0.7087±0.0007 (Fig. 6b). Initial $(^{87}Sr/^{86}Sr)_{357}$ for all the granitoids shows heterogeneity (Table 2) and εNd_{357} decreases from tonalite to granite (Table 3). The granitoids were deformed by D3 of 300–320 Ma old (Dias et al., 2002) and were intruded by three muscovite–biotite granites of 328±9, 319±7 and 315±8 Ma yielded by three whole-rock Rb–Sr isochrons (Gomes, 1996).

Whole-rock oxygen isotope ($\delta^{18}O$) values, obtained for nine representative samples of the studied granitoids, range from +8.60‰ to +10.10‰ (Table 4). The samples with the lowest $\delta^{18}O$ belong to tonalite and have the lowest SiO_2 and the highest Fe_2O_3t. The samples with the highest $\delta^{18}O$ values are of micro-granular enclaves and host granite, suggesting that

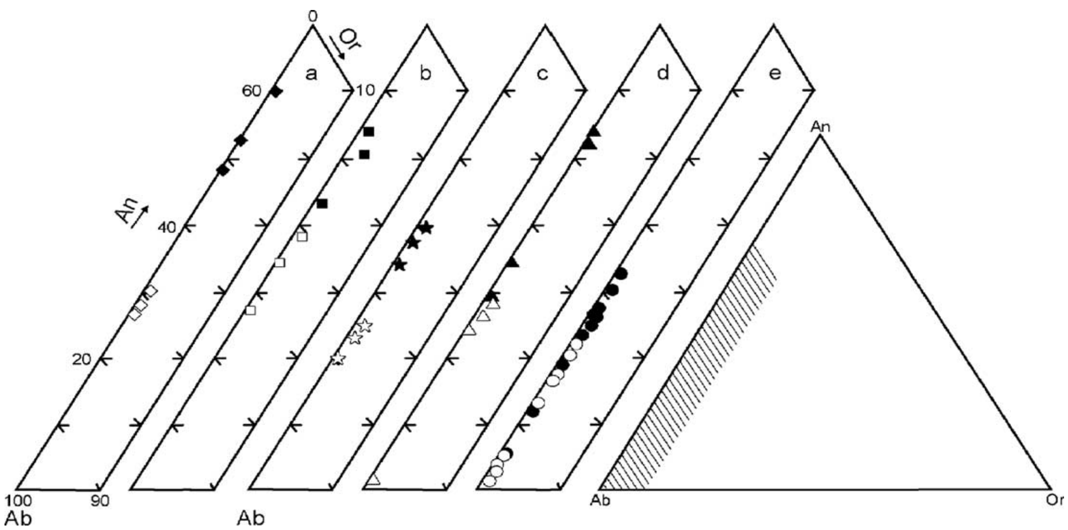

Fig. 7. Plot of plagioclase compositions of granitoids from Rebordelo–Agrochão area. (a) B1, (b) E1, (c) E2, (d) B2 and (e) B3. Symbols as in Fig. 2, but a star was used for E2; closed symbols—cores, and open symbols—rims.

Table 6
Average electron microprobe analyses in wt.% of amphibole of tonalite and sphene of granitoids from Rebordelo–Agrochão, northern Portugal

	Amphibole			Sphene		
	Mgh a	Mgh b	Actinolite	B1	B2	B3
SiO_2	49.09	50.89	53.17	31.46	32.00	31.73
Al_2O_3	6.75	4.46	2.85	2.21	2.46	7.86
TiO_2	0.60	0.34	0.21	35.99	35.50	28.92
FeOt	15.51	13.80	14.28	0.48	0.54	2.06
MnO	0.48	0.44	0.56	0.11	0.08	0.07
MgO	12.23	14.03	14.04	0.11	0.12	0.56
CaO	12.20	11.92	12.02	28.70	29.04	27.88
Na_2O	0.82	0.88	0.33	0.39	0.31	0.29
K_2O	0.57	0.33	0.19	0.07	0.41	0.07
Total	98.25	97.09	97.65	99.52	100.46	99.44
$Mg/(Mg+Fe^{2+})$	0.62	0.69	0.67			

Mgh—magnesiohornblende, a—the least silicic samples, b—the most silicic samples, B1—tonalite, B2—granodiorite, B3—granite, FeOt—total FeO. Analyst: M.E.P. Gomes.

they are due to the high fractionation in the coeval tonalite–granite sequence.

7. Geochemistry of minerals

7.1. Feldspars

Compositions of plagioclase and K-feldspar are given in Table 5. In general, there is a decrease in anorthite content from phenocryst plagioclase to matrix plagioclase. Furthermore, in K-feldspar, orthoclase content tends to increase and Ba content decreases from phenocrysts to matrix, which can indicate a magmatic origin (Long and Luth, 1986). Anorthite content of plagioclase decreases in the sequence tonalite, tonalitic enclave, granodioritic enclave, granodiorite and granite (Table 5, Fig. 7) as the CaO content of whole rock (Fig. 3). Locally, plagioclase is oscillatory zoned in all granitoids, indicating probably disequilibrium melting in the generation of granitoid rocks (Castro, 2001). The crystal shapes of K-feldspar, simple twinning and its zoned euhedral plagioclase inclusions found in the tonalitic and granodioritic enclaves suggest that they have an igneous origin (Vernon and Paterson, 2002).

7.2. Amphibole

Only the biotite–hornblende tonalite B1 contains amphibole. The electron microprobe compositions of amphibole are given in Table 6 and display a wide range of Si pfu, from 7.01 to 7.79 (Fig. 8). Single homogeneous crystals of magnesiohornblende were found in the least silicic and intermediate samples, while the most silicic samples have some zoned crystals with a core of magnesiohornblende and a rim of subsolidus actinolite.

7.3. Biotite

Major and trace element contents of the analysed biotites are given in Table 7. All are Fe^{2+}-biotites

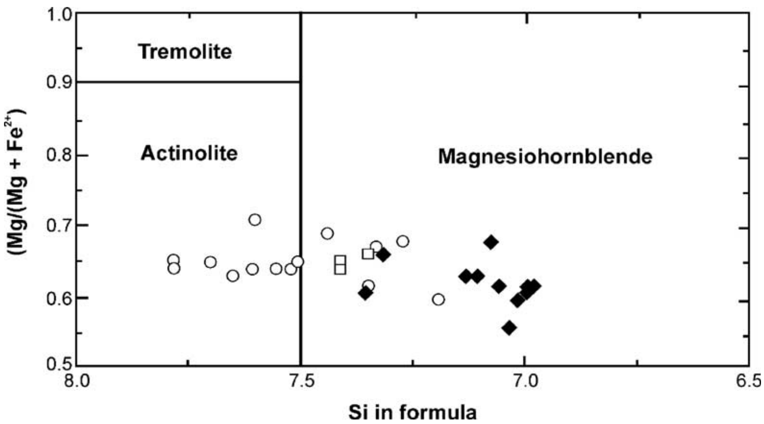

Fig. 8. Classification of compositions of amphiboles from tonalite B1, according to the IMA nomenclature (Leake et al., 1997). Symbols: ◆—the least silicic sample, □—the intermediate sample, ○—the most silicic sample.

according to the nomenclature of Foster (1960). Most biotites correspond to the Al–K-biotite (Nachit et al., 1985) and some biotite compositions from tonalite and granodiorite, and rarely of granite, plot in the field of biotite from calc-alkaline rocks (Fig. 9); a similar conclusion is obtained if they are plotted in the diagrams of Rahman (1994).

The biotites of the studied granitoids show fractionation trends for major and trace elements (Fig. 10). There are increases in Nb, Li, Sn, Rb, Cs, Li/Mg and decreases in Mg and K/Rb from biotite of the most-deformed samples to the biotite of the least-deformed samples of granite (Fig. 11 and Table 7) showing that there is fractionation of biotite in granite with the decrease in the degree of deformation.

7.4. Sphene

Chemical compositions of the analysed sphene are given in Table 6 and fractionation trends are presented in Fig. 12.

Table 7
Average chemical analyses in wt.% and trace elements in ppm of biotite of granitoids from Rebordelo–Agrochão, northern Portugal

	Tonalite	Enclaves		Granodiorite	Granite		
	B1	Tonalitic E1	Granodioritic E2	B2	B3	a	b
SiO_2	36.84	36.34	35.49	36.42	35.67	35.87	35.67
Al_2O_3	16.63	19.12	18.79	17.69	18.58	17.99	18.94
TiO_2	2.69	3.15	3.41	3.00	2.66	2.59	2.52
Fe_2O_3	2.02	1.47	2.27	1.90	1.85	1.87	1.62
FeO	17.78	17.98	17.91	18.91	20.35	20.11	20.96
MnO	0.27	0.08	0.28	0.22	0.23	0.22	0.32
MgO	10.37	8.73	8.68	8.52	7.51	7.55	7.05
CaO	0.08	0.12	0.02	0.06	0.02	0.03	0.04
Na_2O	0.68	0.54	0.59	0.26	0.35	0.37	0.35
K_2O	9.43	9.52	9.45	9.60	9.55	9.61	9.43
Cl	0.06	0.06	0.07	0.06	0.05	0.06	0.05
F	0.30	0.47	0.45	0.36	0.39	0.40	0.37
Total	97.15	97.58	97.41	97.00	97.21	96.67	97.32
O≡Cl	0.01	0.01	0.02	0.01	0.01	0.01	0.01
O≡F	0.13	0.20	0.19	0.15	0.16	0.17	0.16
Total	97.01	97.37	97.20	96.84	97.04	96.49	97.15
Cr	211	252	211	176	136	164	130
V	355	348	535	363	314	338	277
Nb	39	87	111	95	128	100	146
Zn	355	368	403	469	579	599	610
Sn	82	88	109	118	133	132	156
Li	708	493	800	879	1146	1133	1586
Ni	115	109	86	79	71	40	81
Zr	18	109	91	79	81	74	51
Cu	14	*	*	10	8	6	16
Sc	35	44	51	42	34	34	23
Y	55	66	38	65	70	65	73
Sr	24	24	21	20	20	22	19
Ba	470	441	198	408	70	91	56
Rb	891	1095	1039	1115	1358	1320	1464
Cs	32	56	38	52	91	81	112
Ta	6	1	14	9	17	3	28
Ce	31	20	100	75	56	48	81
Nd	9	1	25	20	11	4	13
La	22	23	24	30	25	20	25

a—The most-deformed granite B3, b—the least-deformed granite B3, *below the limit of sensitivity. Analyst: M.E.P. Gomes.

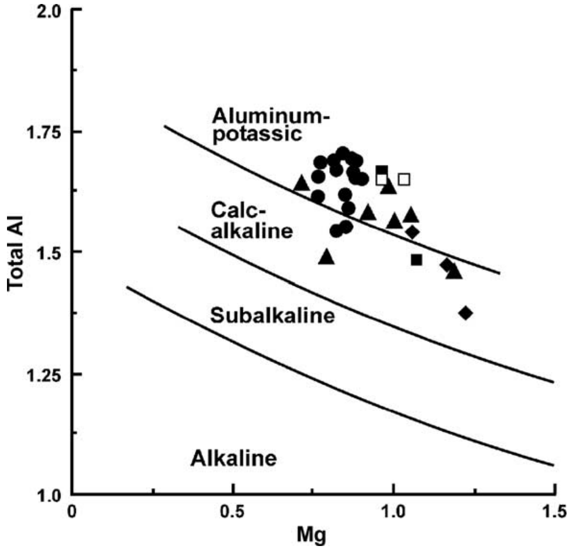

Fig. 9. Total Al versus Mg diagram adapted from Nachit et al. (1985) for biotites of granitoids from Rebordelo–Agrochão area. Symbols as in Fig. 2.

7.5. Thermodynamic conditions

Magnesiohornblende compositions are used, but subsolidus actinolite rims are not taken into account for the calculation of pressure. Crystallization pressure of 2.7 kb is calculated for tonalite from the Al-in-hornblende geobarometer of Schmidt (1992). Crystallization temperature up to 743±40 °C is calculated from the amphibole–plagioclase geothermometer (Holland and Blundy, 1994). Melt temperature is calculated using Zr content of tonalite and the models of Watson and Harrison (1983) and Miller et al. (2003) and values up to 810 and 832 °C, respectively, are obtained, which may correspond to the temperature of extraction of the tonalitic magma. Therefore, they are higher than that obtained from the amphibole–plagioclase geothermometer, which represents the last temperature of equilibrium of the plagioclase–amphibole pair. Temperatures calculated using the Zr thermometers range from 810 to 860 °C for all the granitoid magmas, but a regular decrease in temperature of extraction is not found from tonalite magma to granite magma, probably due to analytical and experimental errors. Melt temperatures are also calculated for all the granitoids containing monazite and using the REE contents and the solubility of monazite (Montel, 1993). Thus, it was applied to most of the granitoids, except to the biotite–hornblende tonalite (B1). There is a decrease in the temperature of extraction from 890 to 876 °C from biotite tonalitic enclave (E1) to biotite–muscovite granite (B3). These temperatures are higher than those estimated from the Zr thermometer. It is likely that at temperatures above 850 °C, monazite is totally dissolved and consequently the REE thermometer must be used with caution (Montel, 1993).

The calculated temperature of 743 °C from the amphibole–plagioclase geothermometer is probably the main crystallization temperature for tonalite. The estimated temperature of crystallization for the biotite–muscovite granite B3 is of 700 °C because the solidus at 1 kb in the system Qz–Ab–Or is 730 to 690 °C with 0 to 1 wt.% F in the melt (Tuttle and Bowen, 1958; Manning, 1981). f_{O2} is estimated from these temperatures, biotite compositions and the work of Burkhard (1991). It ranges from 10^{-17} to 10^{-14} bars, relative to a QFM buffer, from tonalite magma to granite magma. Wt.% F contents in melt, calculated using the data of biotite and experimental results of Icenhower and London (1997), are of 0.08 and 0.14 for tonalite and granite, respectively. Therefore, wt.% F increases from tonalite magma to granite magma.

A pressure of emplacement of 3 kb for enclaves and granodiorite is assumed, because granodiorite B2 contains primary muscovite with significant celadonite component and may have crystallized at about 2.6–3.1 kb (Anderson and Rowley, 1981), and tonalitic and granodioritic enclaves E1 and E2 have compositions plotting between those of tonalite B1 and granodiorite B2 (Fig. 3), which crystallized at about 3 kb. Granite B3 contains sillimanite and the experimental work of Holdaway and Muskhopadhy (1993) suggests that this mineral crystallizes at about 4 kb.

Temperatures estimated from the two-feldspar geothermometer of Elkins and Grove (1990), for the respective pressure, range from 401 to 541 °C for tonalitic and granodioritic compositions and are 263–384 °C for granite, which correspond to temperatures of reequilibrium of feldspars under subsolidus conditions.

8. Petrogenesis

The variation diagrams of peraluminous granitoid rocks from Rebordelo–Agrochão area (Fig. 3), biotite

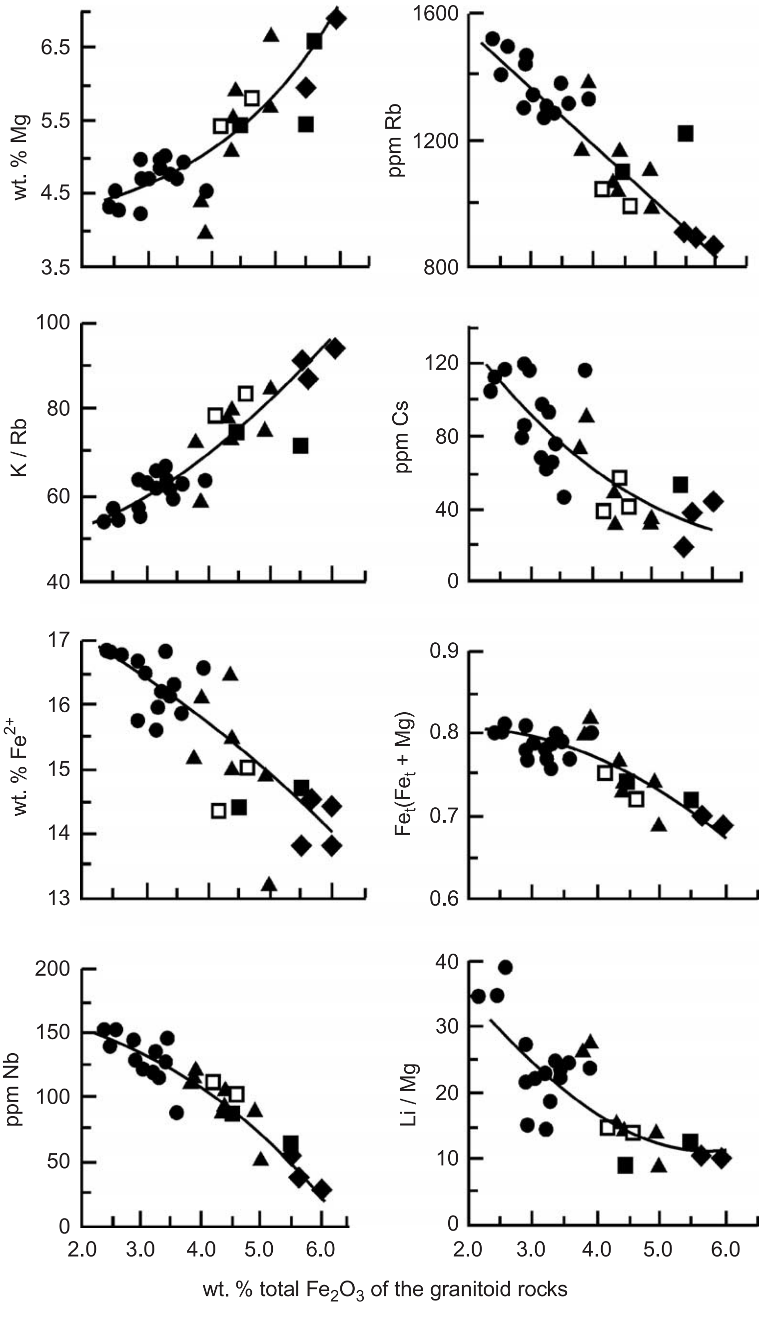

Fig. 10. Variation diagrams for selected major, trace elements and ratios of biotites of granitoids from Rebordelo–Agrochão area. Symbols as in Fig. 2.

(Fig. 10) and sphene (Fig. 12), the subparallel rare earth patterns of granitoids (Fig. 5a) and the decrease in Ca of plagioclase from tonalite to granite and from core to rim (Table 5 and Fig. 7) suggest an AFC model, supported by isotopically heterogeneous data. The variation diagrams for the granite (Fig. 4) and its biotite (Fig. 11) and the subparallel REE patterns for the most-deformed and the least-

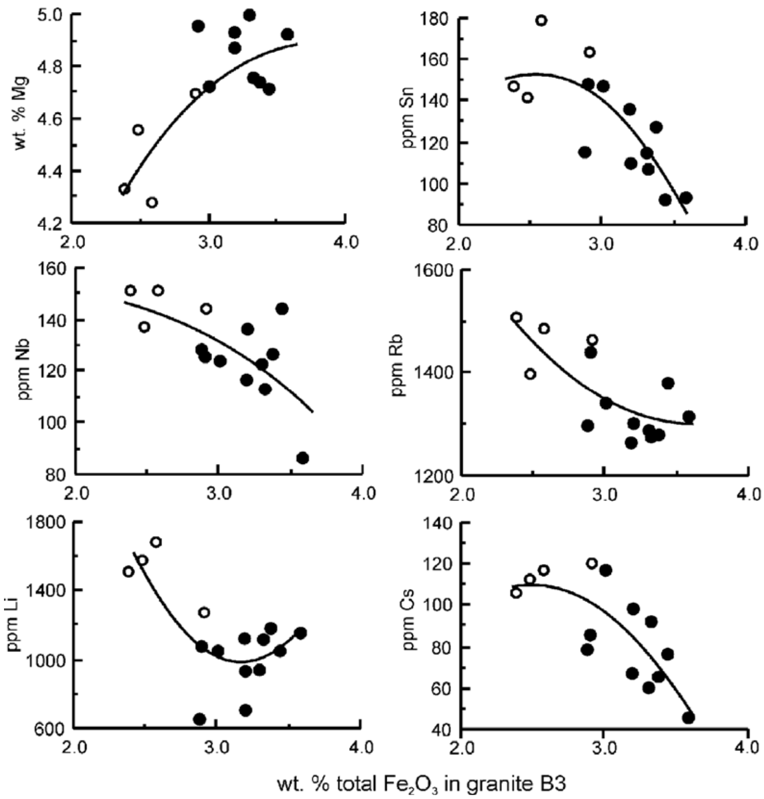

Fig. 11. Variation diagrams for selected major and trace elements of biotites of the most-deformed and the least-deformed samples of granite B3 from Rebordelo–Agrochão area. Symbols as in Fig. 4.

deformed samples of granite (Fig. 5b) suggest an increase in the crystal fractionation with decrease in the degree of deformation.

The decrease in middle and heavy rare earth elements (HREE) from tonalite to granite (Fig. 5a) and from the most-deformed to the least-deformed samples of granite (Fig. 5b) is probably due to fractionation of apatite as evidenced by the decrease in P_2O_5 from tonalite to granite (Table 1). The depletion in HREE may also be due to fractionation of some zircon, which is supported by the decrease in Zr from tonalite to granite (Table 1). The decrease in LREE from tonalite to granite is mainly attributed to fractionation of allanite, sphene and monazite. Within

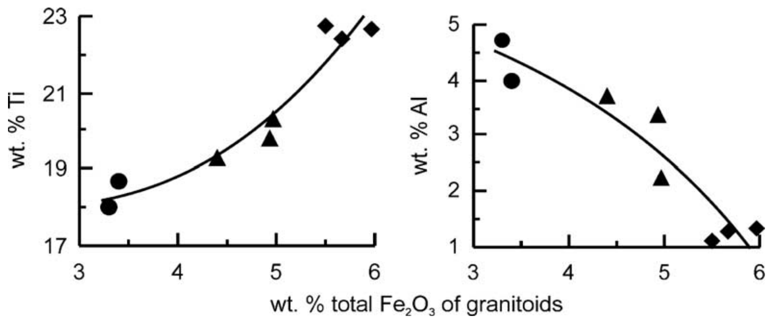

Fig. 12. Variation diagrams for Ti and Al of sphene of granitoid rocks from Rebordelo–Agrochão area. Symbols as in Fig. 2.

granite, from the most- to the least-deformed samples, the decrease in LREE may be explained by fractionation of sphene and monazite.

Modelling of major and trace elements shows that granodioritic enclaves, granodiorite and the most- and least-deformed samples of granite are compatible with a fractional crystallization model. Fractional crystallization of magnesiohornblende, plagioclase, biotite, ilmenite and quartz of the tonalitic magma would have taken place (Table 8). In this modelling, the average composition of tonalite was selected as the parental magma, while the average composition of granodioritic enclaves, granodiorite, and the three most-deformed and the two least-deformed samples of granite were selected as residual liquids. The least squares regression method was used to model the major elements using the compositions of amphibole, biotite and ilmenite determined by electron microprobe in tonalite and pure anorthite, albite and quartz. The sum of the squares of the residuals ($\sum R^2$) is always <0.63. The anorthite content of the plagioclase of the cumulate is always similar to the highest anorthite content of plagioclase of the tonalite. During fractional crystallization, there was a decrease in the weight fraction of melt remaining (FR) and in the percentage of magnesiohornblende and plagioclase, and an increase in the percentage of biotite in the cumulate (Fig. 13). The tonalitic enclave could not be modelled, because it has a composition close to that of parental magma.

The average contents of Rb, Sr and Ba were used to evaluate fractionation of these granitic rocks. The distribution coefficients for Sr given by Peccerillo et al. (1994) for granodiorites and for Rb and Ba for tonalites were used. The modal compositions of cumulate and FR based on calculations involving

Table 8
Results of the fractional crystallization modelling of granitoids from Rebordelo–Agrochão, northern Portugal

	Determined parent tonalitic magma B1	Calculated composition of parental magma for			
		Granodioritic enclave E2	Granodiorite B2	Granite B3 (a)	Granite B3 (b)
SiO_2	62.64	63.00	62.60	62.70	62.70
TiO_2	0.82	0.80	0.70	0.80	0.60
Al_2O_3	16.78	16.60	16.70	16.80	16.80
Fe_2O_3t	5.76	5.90	5.90	5.80	5.70
MgO	3.16	2.80	2.90	3.10	3.30
CaO	3.99	4.50	4.10	4.00	4.00
Na_2O	3.00	2.90	3.10	3.00	3.00
K_2O	3.86	3.40	4.00	3.90	3.90
FR		0.767±0.066	0.745±0.032	0.564±0.138	0.462±0.168
$\sum R^2$		0.63	0.15	0.05	0.01
Modal composition of cumulate					
Quartz		–	–	13.3±6.9	13.6±6.5
Plagioclase		49.6±19.8	47.2±19.5	42.0±8.6	42.5±7.3
Amphibole		46.6±9.8	26.4±4.6	15.4±3.9	14.3±4.1
Biotite		–	26.4±4.3	29.4±6.9	29.6±5.8
Ilmenite		3.8±2.5	–	–	–
An % of plagioclase		49.1±15.4	50.8±2.1	53.0±2.0	51.5±6.2

Composition of residual melts (ppm)	deter.	calc.	deter.	calc.	deter.	calc.	deter.	calc.	deter.
Sr	278	213	225	212	208	183	165	155	129
Ba	642	774	685	584	659	510	483	467	431
Rb	207	267	244	230	251	218	293	221	295

(a) The most-deformed granite B3, (b) the least-deformed granite B3. FR=weight fraction of melt remaining during fractional crystallization, $\sum R^2$=sum of the squares of the residuals, –= not fractionated, deter.=determined, calc.=calculated.

major elements are used. The results based on the Rayleigh fractionation equation are used in the model, because they are closer to the analytical data than those based on equilibrium crystallization. During fractional crystallization, Ba and Sr decrease and Rb/Sr increases (Fig. 13).

Although the model seems to indicate a fractional crystallization process relating tonalite, granodioritic enclave, granodiorite and granite, an open system must also be considered because the granite has the highest initial $^{87}Sr/^{86}Sr$ ratio (Table 2 and Fig. 6b) and the lowest $\varepsilon_{Nd}(t)$ (Table 3). $(^{87}Sr/^{86}Sr)_{357}$ increases from 0.7070–0.7074 for tonalite to 0.7086–0.7090 for granite (Table 2), suggesting that assimilation of metasediments was contemporaneous to the fractional crystallization.

The AFC model was tested using the equation proposed by De Paolo (1981b), Rb, Sr and $(^{87}Sr/^{86}Sr)_0$ values of the least silicic sample of tonalite B1 and assuming that the assimilated country rock had Rb=204 ppm, Sr=77 ppm and $(^{87}Sr/^{86}Sr)_0$=0.7201, which are the values reported by Beetsma (1995) for two Silurian schists with a similar composition of the schist of the studied area. $^{87}Sr/^{86}Sr$ was calculated for 386 Ma, the age yielded by the whole-rock Rb–Sr isochron defined for the B1, B2 and B3 granitoids (Fig. 6a). The model for this age shows that enclaves, granodiorite and granite could not have been formed by this process, which is attributed to the fact that this age is not supported by field work and resulted from the heterogeneity of Rb–Sr data due to loss during deformation. If 357

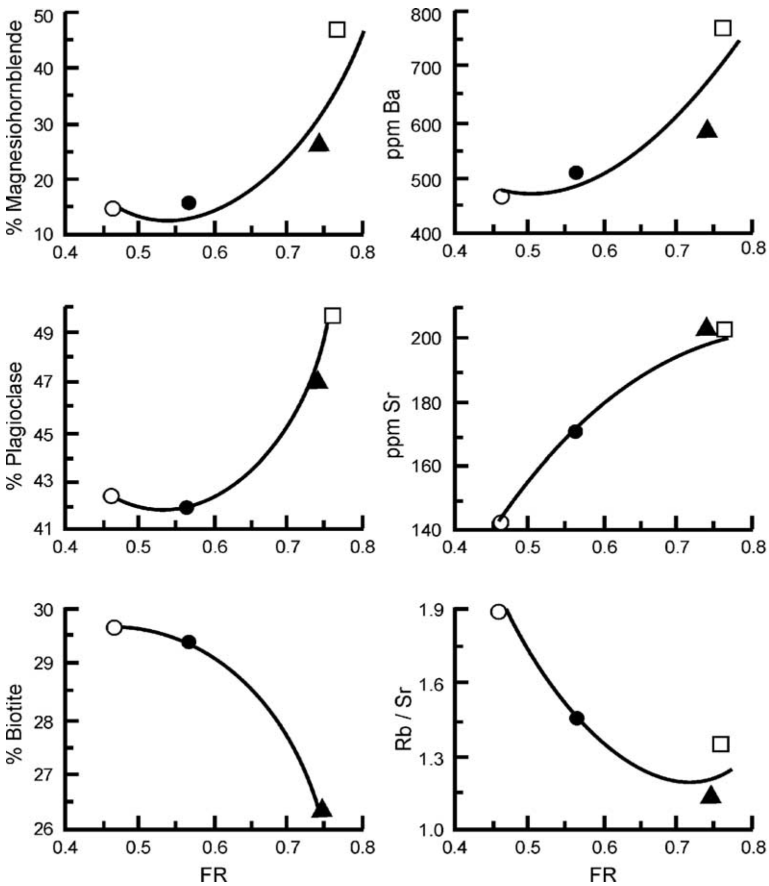

Fig. 13. Plot of modal magnesiohornblende, plagioclase and biotite and of calculated Ba, Sr and Rb/Sr in granitoid rocks from Rebordelo–Agrochão versus the weight fraction of melt remaining during fractional crystallization (FR). Symbols as in Fig. 2, but ●—the most-deformed samples and ○—the least-deformed samples of granite B3.

Ma age (Fig. 6b) is considered to be the minimum emplacement age for the granitoid magma and simultaneous assimilation of metasedimentary materials took place, Fig. 14 provides the support for the hypothesis that tonalitic and granodioritic enclaves, granodiorite and granite have been generated by an AFC process.

The positive correlation between $\delta^{18}O$ and SiO_2 and the negative correlation between $\delta^{18}O$ and total Fe_2O_3 of granitoids (Table 4) are expected in fractional crystallization process (Table 8). $\delta^{18}O$ values of +8.60–+9.08 ‰ in tonalite, +9.30–+9.69 ‰ in granodiorite and +9.34–+10.10 ‰ in granite are in accordance with the AFC process (Fig. 14). Subsolidus temperatures, ranging between 541 and 263 °C from tonalite to granite, were estimated from the two-feldspar geothermometer, suggesting that feldspars behaved as an open system. Hence, it is possible that these feldspar-rich rocks have their whole-rock $\delta^{18}O$ values modified due to oxygen-isotope exchange at subsolidus temperature between feldspar and probably quartz. However, hydrothermal alteration of feldspars would decrease $\delta^{18}O$ values of these granitoid rocks. Therefore, the increase in 1.5 ‰ of $\delta^{18}O$ values from tonalite to granite is attributed to the AFC mechanism (De Paolo, 1981b; Blattner et al., 2002). Furthermore, tonalitic and granodioritic enclaves have $\delta^{18}O$ values close to those of granodiorite and granite (Table 4), suggesting that they were probably generated by a source of similar $\delta^{18}O$ composition.

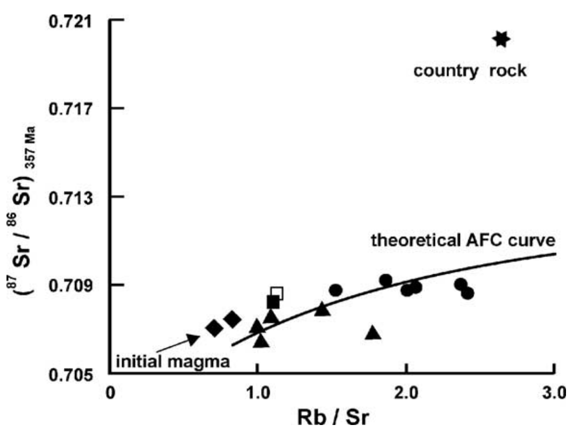

Fig. 14. $(^{87}Sr/^{86}Sr)_{357Ma}$ variation with Rb/Sr of granitoids from Rebordelo–Agrochão area. The theoretical AFC curve (De Paolo, 1981b) with r=0.3 is also shown. Symbols as in Fig. 2.

The tonalite contains amphibole, sphene, allanite and magnetite and probably represents a hybrid magma derived from an enriched and isotopically heterogeneous source. The tonalite may have been derived by the interaction of a mantle magma and crustal materials supported by the $(^{87}Sr/^{86}Sr)_{357}$ ratio of 0.7072, εNd_{357} of −4.3 and $\delta^{18}O$ of +8.60–+9.08‰.

These granitoids from Rebordelo–Agrochão are hybrid (mantle±crust). The tonalite, microgranular enclaves and granodiorite are of H_{CA} type generated and emplaced during an active subduction zone and the granite is an C_{CI} type, as crustal intrusive according to Barbarin classification (1999). The intrusions of magmas were controlled by the NW–SE regional Laza–Rebordelo dextral shear zone.

9. Conclusions

(1) Granitoids from Rebordelo–Agrochão comprise deformed syntectonic biotite–hornblende tonalite, biotite granodiorite and biotite–muscovite granite, which intruded concordantly Silurian metasedimentary rocks and show structures parallel to the NW–SE extense Laza–Rebordelo dextral shear zone.

(2) The granitoids are peraluminous and show trends of fractionation for oxides and trace elements. There is a decrease in $\sum$REE, but mainly in LREE, and increase in the negative Eu anomaly from tonalite to granite. The granitoids define a whole-rock Rb–Sr isochron, which yields an age of 386±9 Ma and an initial $^{87}Sr/^{86}Sr$ ratio of 0.7063±0.0005. The whole-rock Rb–Sr isochron for the least-deformed samples of granite gives the age of 357±9 Ma and initial $^{87}Sr/^{86}Sr$ of 0.7087±0.0007, which is considered the minimum emplacement age of the granitoid magma.

(3) The microgranular enclaves fit the fractionation trends for major and trace elements, plotting between tonalite and host granite compositions. Enclaves and the other granitoids fit a whole-rock Rb–Sr errorchron, which yields the same age and initial $^{87}Sr/^{86}Sr$ ratio given by the isochron for tonalite, granodiorite and granite, i.e., 386 Ma.

(4) Biotites and sphenes of these granitoids and microgranular enclaves show trends of fractionation for major and trace elements.
(5) The most- and the least-deformed samples of granite and also their biotites show trends of fractionation for major and trace elements. All REE contents decrease and the negative Eu anomaly increases from the most- to the least-deformed sample of granite.
(6) The granitoids and enclaves from Rebordelo–Agrochão are the product of in situ fractional crystallization of tonalitic magma controlled by separation of magnesiohornblende, plagioclase, biotite, ilmenite and quartz, but simultaneous assimilation of metasedimentary materials also took place as suggested by initial $(^{87}Sr/^{86}Sr)_{357}$ ratio, εNd_{357} and $\delta^{18}O$ values . The AFC model was successfully tested. The tonalite may have been derived by the interaction of a mantle magma and crustal materials.
(7) Pressure of 2.7 kb and the temperature of 743 ± 40 °C are estimated for the main crystallization stage. Feldspars from tonalite, granodiorite and microgranular enclaves reequilibrated at 401–541 °C and those from granite reequilibrated at 263–384 °C, mainly under subsolidus conditions. Actinolite in tonalite crystallized under subsolidus conditions.

Acknowledgements

This paper corresponds to part of the PhD thesis of M.E.P. Gomes. Thanks are due to Dr. J. Esson for the XRF and microprobe facilities provided at the Department of Earth Sciences, University of Manchester, U.K.; Dr. S. J. Parry for the facilities at the Nuclear Reactor, Ascot, U.K.; Dr. M. Whitehouse and Mr. R. Godwin for the Rb–Sr and Sm–Nd isotopic data obtained at the Department of Earth Sciences, Oxford, U.K.; Prof. F. J. Longstaffe for the oxygen isotope analyses obtained at the Department of Earth Sciences, University of Western Ontario, Canada. Thanks are also due to Prof. J. Machado Leite and Dr. J.M. Farinha Ramos for microprobe facilities in the Geologic and Mining Institute, IGM, Oporto, Portugal, Prof. L. Carvalho and Mr. A. Duarte for the determinations by atomic absorption and wet chemical analyses at the Department of Chemistry, UTAD, Vila Real, Portugal. Funding was provided to M.E.P. Gomes by a grant from ex. I.N.I.C., Portugal. This research was carried out in the programme of Geosciences Centre, University of Coimbra. The critical reviews by Prof. J.-M. Montel and Prof. V.P. Ferrreira are gratefully acknowledged.

References

Anderson, J.L., Rowley, M.C., 1981. Synkinematic intrusion of peraluminous and associated metaluminous granitic magmas—Whipple Mountains, California. Can. Mineral. 19, 83–102.

Azevedo, M.R., Nolan, J., 1998. Hercynian late-post-tectonic granitic rocks from the Fornos de Algodres area (northern Central Portugal). Lithos 44, 1–20.

Barbarin, B., 1999. A review of the relationships between granitoid types, their origins and their geodynamic environments. Lithos 46, 1605–1626.

Beetsma, J.J., 1995. The late Proterozoic/Paleozoic and Hercynian crustal evolution of the Iberian Massif, Northern Portugal. Unpublished PhD thesis, Faculty of Earth Sciences, Vrije Univ., Amsterdam, 233 pp.

Blattner, P., Abart, R., Adams, C.J., Faure, K., Hui, L., 2002. Oxygen isotope trends and anomalies in granitoids of the Tibetan plateau. J. Asian Earth Sci. 21-3, 241–250.

Brown, G.C., Hughes, D.J., Esson, J., 1973. New X.R.F. data retrieval techniques and their application to U.S.G.S. standard rocks. Chem. Geol. 11, 223–229.

Burkhard, D.J.M., 1991. Temperature and redox path of biotite-bearing intrusives: a method of estimation applied to S- and I-type granites from Australia. Earth Planet. Sci. Lett. 104, 89–98.

Castro, A., 2001. Plagioclase morphologies in assimilation experiments. Implications for disequilibrium melting in the generation of granodiorite rocks. Mineral. Petrol. 71, 31–49.

Debon, F., Le Fort, P., 1983. A chemical–mineralogical classification of common plutonic rocks and associations. Trans. R. Soc. Edinb. Earth Sci. 73, 135–149.

De Paolo, D.J., 1981a. Neodymium isotopes in the Colorado Front Range and crust–mantle evolution in the Proterozoic. Nature 291, 193–196.

De Paolo, D.J., 1981b. Trace element and isotopic effects of combined wall rock assimilation and fractional crystallization. Earth Planet. Sci. Lett. 52, 177–184.

Dias, G., Leterrier, J., 1994. The genesis of felsic–mafic plutonic associations: a Sr and Nd isotopic study of the Hercynian Braga granitoid massif (northern Portugal). Lithos 32, 207–223.

Dias, G., Simões, P.P., Ferreira, N., Leterrier, J., 2002. Mantle and crustal sources in the genesis of late- Hercynian granitoids (NW Portugal): geochemical and Sr–Nd isotopic constraints. Gond. Res. 5-2, 287–305.

Elkins, L.T., Grove, T.L., 1990. Ternary feldspar experiments and thermodynamic models. Am. Mineral. 75, 544–559.

Ferreira, N., Iglésias, M., Noronha, F., Pereira, E., Ribeiro, A., Ribeiro, M.L., 1987. Granitóides da zona Centro-Ibérica e seu enquadramento geodinâmico. In: Bea, F., Carmina, A., Gonzalo, J.C., Plaza, M.L., Rodrigues, J.M.L. (Eds.), Geologia de los granitoids y rocas associadas del Macizo Hespérico, Libro Homenage a L.C.G. Figueirola. Editorial Rueda, Madrid, pp. 37–53.

Foster, M.D., 1960. Interpretation of the composition of trioctahedral micas. U.S. Geol. Surv. Prof. Paper 354-B, 1–49.

Frost, B.R., Barnes, C.G., Collins, W.J., Arculus, R.J., Ellis, D.J., Frost, C.D., 2001. A geochemical classification for granitic rocks. J. Petrol. 42, 2033–2048.

Gomes, M.E.P., 1996. Mineralogia, Petrologia e Geoquímica das rochas granitóides da área de Rebordelo-Bouça-Torre de D.Chama-Agrochão e as mineralizações associadas. Unpublished PhD thesis, University of Trás-os-Montes e Alto Douro, Vila Real, p. 323.

Haskin, L.A., Haskin, M.A., Frey, F.A., Wildman, T.R., 1968. Relative and absolute terrestrial abundances of the rare earths. In: Ahrens, L.H. (Ed.), Origin and Distribution of the Rare Elements, vol. 1. Pergamon, Oxford, pp. 889–911.

Holdaway, M.J., Muskhopadhy, B., 1993. A reevaluation of the stability relations of andalusite: thermodynamic data and phase diagram for the aluminum silicates. Am. Mineral. 78, 298–315.

Holland, T., Blundy, J., 1994. Non ideal interactions in calcic amphiboles and their bearing on amphibole–plagioclase thermometry. Contrib. Mineral. Petrol. 116, 433–447.

Icenhower, J.P., London, K., 1997. Partitioning of fluorine and chlorine between biotite and granitic melt: experimental calibration at 200 Mpa H_2O. Contrib. Mineral. Petrol. 127, 17–29.

Leake, B.E., Woolley, A.R., Arps, C.E.S., Birch, W.D., Gilbert, M.C., Grice, J.D., Hawthorne, F.C., Kato, A., Kisch, H.J., Krivovichev, V.G., Linthout, K., Laird, J., Mandarino, J.A., Maresch, W.V., Nickel, E.H., Rock, N.M.S., Schumacher, J.C., Smith, D.C., Stephenson, N.C.N., Ungaretti, L., Whittaker, E.J.W., Youzhi, G., 1997. Nomenclature of amphiboles: report of the subcommittee on amphiboles of the International Mineralogical Association, Commission on new minerals and mineral names. Can. Mineral. 35, 219–246.

Le Bas, M.J., Streckeisen, A.L., 1991. The IUGS systematics of igneous rocks. J. Geol. Soc. (Lond.) 148, 825–833.

Lécolle, M., Derré, C., Noronha, F., Roger, G., 1981. Distribution des concentrations Sn-W dans le Nord du Trás-os-Montes (Portugal); typologies gîtologiques et mineralógiques. Rappot final-ATP du CNRS "Formation et distribution des gisements—1978", décision d'aide, vol. 3548, 19 pp.

Long, P.E., Luth, W.C., 1986. Origin of K-feldspar megacrysts in granitic rocks: implications of a partitioning model for barium. Am. Mineral. 71, 367–375.

Ludwig, K.P., 1990. Isoplot: a plotting and regression program for radiogenic-isotope data, for IBM-PC compatible computers. US Geological Survey Open File Report, vol. 85, p. 513.

Manning, D.A.C., 1981. The effect of fluorine on liquids phase relationships in the system Qz–Ab–Or with excess water at 1 Kb. Contrib. Mineral. Petrol. 76, 206–215.

Matte, Ph., 1986. La chaîne varisque parmi les chaînes paléozoiques péri atlantiques, modèle d'évolution et position des grands blocs continentaux au Permo–Carbonifére. Bull. Soc. Géol. 2, 9–24.

Michard, A., Gurriet, P., Soudant, M., Albarede, F., 1985. Nd isotopes in French Phanerozoic shales: external versus internal aspects of crustal evolution. Geochim. Cosmochim. Acta 49, 601–610.

Miller, C., Meschter, S., Mapes, R., 2003. Hot and cold granites?: implications of zircon saturation temperatures and preservation of inheritance. Geology 31-6, 529–532.

Montel, J.-M., 1993. A model for monazite/melt equilibrium and application to the generation of granitic magmas. Chem. Geol. 110, 127–146.

Nachit, H., Razafimahefa, N., Stussi, J.M., Carron, J.P., 1985. Composition chimique des biotites et typologie magmatique des granitoides. C.R. Acad. Sci. Paris 301 (11), 813–818.

Neiva, A.M.R., 1981. Geochemistry of hybrid granitoid rocks and of their biotites from central northern Portugal and their petrogenesis. Lithos 14, 149–153.

Neiva, A.M.R., Gomes, M.E.P., 2001. Diferentes tipos de granitos e seus processos petrogenéticos: granitos hercínicos portugueses. Mem. Acad. Ciências de Lisboa XXXIX, 53–95.

Pankhurst, R.J., O'Nions, R.K., 1973. Determination of Rb–Sr and $^{87}Sr/^{86}Sr$ ratios of some standard rocks and evaluation of X-ray fluorescence spectrometry in Rb–Sr geochemistry. Chem. Geol. 12, 127–136.

Peccerillo, A., Pinarelli, L., Del Moro, A.B., Rotura, A., 1994. Interaction between mafic and salic magmas in granitoid plutons as inferred from geochemical and Sr–Nd isotopic study of enclaves and host granitoids from Cima d'Asta, Southern Alps, Italy. Per. Mineral. 63, 93–111.

Rahman, A.A.M., 1994. Nature of biotites from alkaline, calk-alkaline, and peraluminous magmas. J. Petrol. 35, 525–541.

Ribeiro, A., 1974. Contribuition l'étude tectonique de Trás-os-Montes Oriental. Mem. Serv. Geol. Port. 24 (168 pp.).

Ribeiro, A., Quesada, C., Dallmeyer, R.D., 1990. Geodynamic evolution of the Iberian Massif. In: Dallmeyer, R.D., Martinez Garcia, E. (Eds.), Pre-Mesozoic Geology of Iberia. Springer-Verlag, Berlin, pp. 399–409.

Schmidt, M.W., 1992. Amphibole composition in tonalite as a function of pressure: an experimental calibration of the Al in hornblende barometer. Contrib. Mineral. Petrol. 110, 304–310.

Silva, M.M.V.G., Neiva, A.M.R., 2000. Geochemistry of Hercynian peraluminous granites and their minerals from Carregal do Sal-Nelas–Lagares da Beira area, Central Portugal. Chem. Erde 59, 329–349.

Silva, M.M.V.G., Neiva, A.M.R., Whitehouse, M.J., 2000. Geochemistry of enclaves and host granites from the Nelas area, Central Portugal. Lithos 50, 153–170.

Tuttle, O.F., Bowen, N.L., 1958. Origin of granite in the light of experimental studies in the system $NaAlSi_3O_8$–$KAlSi_3O_8$–SiO_2–H_2O. Geol. Soc. Am., Mem. 74, 1–145.

Vernon, R.H., Paterson, S.R., 2002. Igneous origin of K-feldspar megacrysts in deformed granite of the Papoose Flat Pluton, California, USA. Electron. Geosci. (Published online, 16 July 2002).

Watson, E.B., Harrison, T.M., 1983. Zircon saturation revisited: temperature and composition effects in a variety of crustal magma types. Earth Planet. Sci. Lett. 64, 295–304.